

# Development and testing of EUV multilayer coatings for the Atmospheric Imaging Assembly instrument aboard the Solar Dynamics Observatory

Regina Soufli<sup>\*1</sup>, David L. Windt<sup>2</sup>, Jeff C. Robinson<sup>1</sup>, Sherry L. Baker<sup>1</sup>, Eberhard Spiller<sup>1</sup>, Franklin J. Dollar<sup>3</sup>, Andrew L. Aquila<sup>3</sup>, Eric M. Gullikson<sup>3</sup>, Benjawan Kjornrattanawanich<sup>4</sup>, John F. Seely<sup>5</sup>, Leon Golub<sup>6</sup>

<sup>1</sup>Lawrence Livermore National Laboratory, 7000 East Avenue, Livermore, CA 94550, USA

<sup>2</sup>Columbia Astrophysics Laboratory, New York, NY 10027, USA

<sup>3</sup>Lawrence Berkeley National Laboratory, Berkeley, CA 94720, USA

<sup>4</sup>Universities Space Research Association, National Synchrotron Light Source, Beamline X24C, Brookhaven National Laboratory, Upton, NY 11973, USA

<sup>5</sup>Space Science Division, Naval Research Laboratory, Washington, DC 20375, USA

<sup>6</sup>Harvard-Smithsonian Center for Astrophysics, Cambridge, MA 02138, USA

## ABSTRACT

We present experimental results on the development and testing of the extreme ultraviolet (EUV) reflective multilayer coatings that will be used in the Atmospheric Imaging Assembly (AIA) instrument. The AIA, comprising four normal-incidence telescopes, is one of three instruments aboard the Solar Dynamics Observatory mission, part of NASA's Living with a Star program, currently scheduled for launch in 2008. Seven different multilayer coatings will be used, covering the wavelength region from 93.9 to 335.4 Å.

**Keywords:** Solar Dynamics Observatory, Atmospheric Imaging Assembly, EUV, multilayer coatings, solar physics

## 1. INTRODUCTION

The AIA instrument aboard the Solar Dynamics Observatory (Ref.1) is designed to provide an unprecedented view of the solar corona, taking images that span at least 1.3 solar diameters in multiple wavelengths nearly simultaneously, at a resolution of 1 arcsecond, field of view exceeding 41 arcminutes and at a cadence of 10 seconds or better. AIA will produce essential data for quantitative studies of the evolving coronal magnetic field and its plasma. These data will be used to significantly improve the understanding of the physics behind the activity displayed by the Sun's atmosphere, which drives space weather in the heliosphere and in planetary environments. The AIA is composed of four telescopes, each including a primary-secondary pair of mirrors operating at near-normal angles of incidence. Each telescope produces images at two different wavelengths accomplished by two different multilayer coatings acting as Bragg reflectors, deposited across two respective D-shaped areas on each mirror. In this manner, imaging at a total of eight channels -seven in the EUV and one in the UV range- is achieved. In this talk we are discussing the development of multilayer coatings for the seven EUV (93.9, 131, 171.1, 193.5, 211.3, 303.8 and 335.4 Å) channels of the AIA instrument, shown in Figures 1(a), 2. EUV wavelengths were selected in order to observe the solar corona at specific temperatures corresponding to Fe and He ion lines, as shown in Table 1 and Figure 2. It is worthwhile noting that two of the AIA channels (93.9, 131 Å) have never been implemented in earlier solar missions and thus will be observed for the very first time with AIA. Two additional AIA wavelengths (211.3, 335.4 Å) were not included in the earlier SOHO and TRACE missions. The predicted response from the EUV multilayer coatings for AIA is plotted in Figure 2, combined with the transmission of the Zr and Al filters used in the instrument. The pairing of wavelengths in each telescope is such that either the Zr or the Al filter is sufficient for selection of one of the wavelengths in the pair and suppression of the

---

\* [regina.soufli@llnl.gov](mailto:regina.soufli@llnl.gov); phone 925-422-6013; fax 925-423-1488

other, with the exception of the 193/211 Å telescope where both wavelengths fall under the Al filter transmission range: in this case a hardware shutter will be used as wavelength selector, as is illustrated in Figure 1.

All Mo/Si-based multilayer coatings for AIA (131, 171.1, 193.5, 211.3 Å) were produced at Lawrence Livermore National Laboratory (LLNL), with EUV reflectance characterizations at beamline 6.3.2. of the Advanced Light Source synchrotron at Lawrence Berkeley National Laboratory (LBNL). The Mo/Y (93.9 Å) and SiC/Mg (303.8, 335.4 Å) coatings were produced at the Columbia Astrophysics Lab (CAL) with EUV reflectance characterizations using the CAL laser-produced EUV source reflectometer, and at beamline X24A of the National Synchrotron Light Source (NSLS), at Brookhaven National Laboratory. Stress measurements for all multilayer coatings discussed in Section 2 of this manuscript were performed at LLNL.

Multilayer film parameters for each channel have been uniquely optimized to satisfy criteria for peak reflectivity (throughput), suppression of nearby emission lines, lifetime stability and stress properties. Another crucial requirement for efficient AIA imaging is meeting the wavelength specifications across each multilayer-coated flight optic pair, which in turn depends on precise thickness control of the multilayer thin film across each curved mirror surface. Experimental results on all aforementioned aspects of the EUV multilayer optics for AIA are presented in this manuscript.

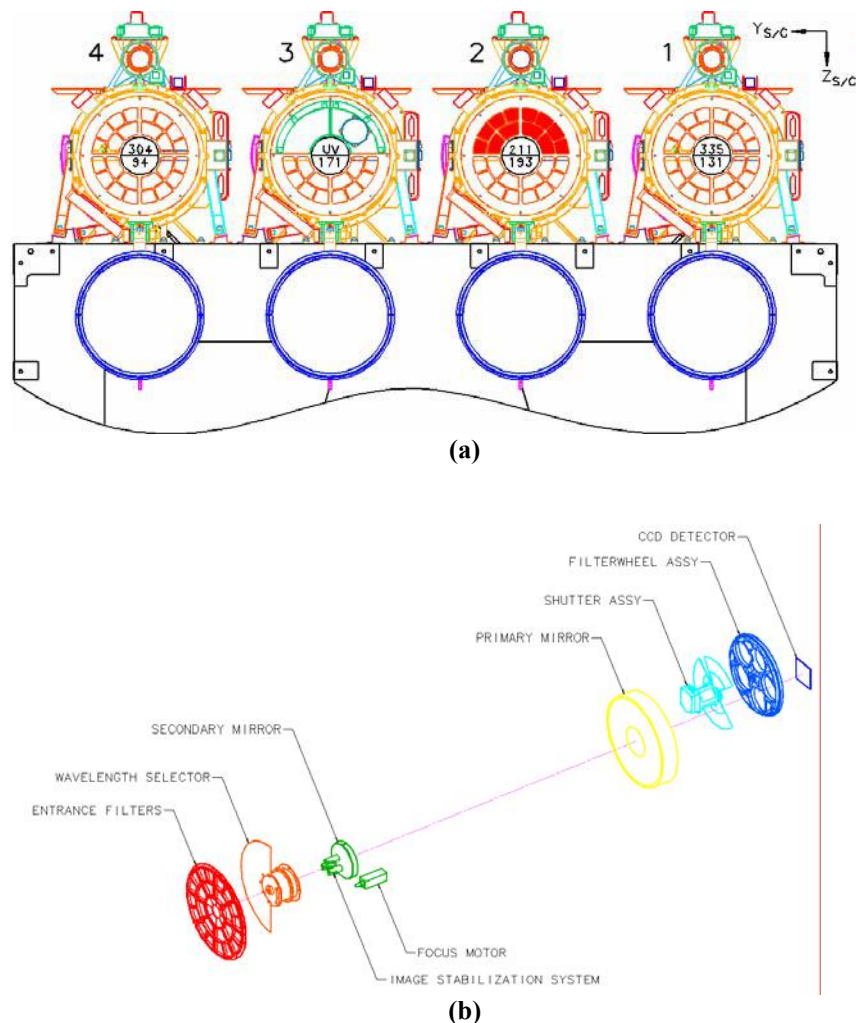


**Figure 1:** (a) Schematic drawing of the front view of the four AIA telescopes with their shutters open. Each telescope is shown with two wavelength channels and a dedicated guide telescope on top. All wavelength units are Angstroms. (b) Interior components of each telescope. Drawings are courtesy of Lockheed Martin Solar and Astrophysics Lab (LMSAL).

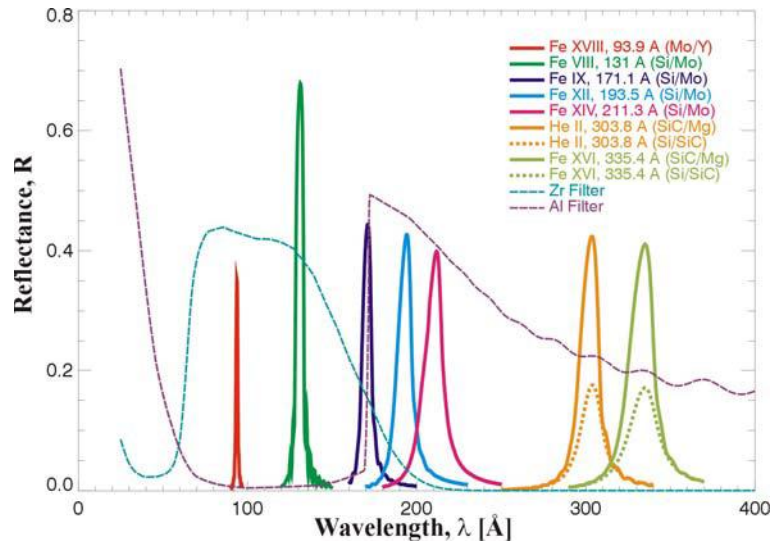


Figure 2: Summary of predicted multilayer reflectance and filter transmission of the AIA instrument.

Channel, $\lambda$	Multilayer	Bandwidth, FWHM, $\Delta\lambda$	Ion line(s)	Region of Solar Atmosphere	Log (T)
335.4 Å	SiC/Mg	14 Å	Fe XVI	Active-region corona	6.4
303.8 Å	SiC/Mg	13 Å	He II	Chromosphere, transition region	4.7
211.3 Å	Mo/Si	11.0 Å	Fe XIV	Active-region corona	6.3
193.5 Å	Mo/Si	9.7 Å	Fe XII, XXIV	Corona and hot flare plasma	6.1, 7.3
171.1 Å	Mo/Si	7.4 Å	Fe IX	Quiet corona, upper transition region	5.8
131.0 Å	Mo/Si	4.8 Å	Fe XX, XXIII	Flaring regions	7.0, 7.2
93.9 Å	Mo/Y	1.1 Å	Fe XVIII	Flaring regions	6.8

Table 1: Summary of EUV wavelengths with corresponding ion lines and temperatures (T) planned for the AIA instrument. The bandwidth values are based on experimental performance of the multilayer coatings discussed later in this manuscript. Part of the material in this Table is courtesy of LMSAL.

## 2. EXPERIMENTAL RESULTS

### 2.1 Multilayer deposition and EUV reflectance characterization facilities

All Mo/Si multilayers on Si wafer and curved AIA substrates discussed in this manuscript were deposited at LLNL in a DC-magnetron sputtering system which has been described in detail in Ref. 2. Briefly, the deposition chamber has planar geometry with a radius of 1 m and allows the coating of large optics (four optics of up to 470 mm in diameter can be

accommodated in a single deposition run) and the off-center mounting and spinning of optics with the possibility of graded coatings. In this manner, both AIA primary and secondary mirrors for a given wavelength channel are coated in a single deposition. The tool has a “sputter down” geometry with five sputtering targets available. For the Mo/Si multilayers discussed in this paper the Mo source is operated at a power of 800 W and Si at 2000 W. Base pressure was maintained at  $10^{-7}$  Torr during the deposition run, and the process gas (Ar) pressure was  $10^{-3}$  Torr. During a multilayer deposition run, the deposition platter is rotating under the sources at speeds in the order of 1 rpm, while each substrate is simultaneously spinning at 400 rpm around its center in order to average out spatial variations of the sputtering sources. To achieve the desired multilayer thickness profile in the radial (lateral) direction for a given flat or curved substrate, the platter speed is modulated as each substrate passes under the Si and Mo targets. A detailed computer model is implemented at LLNL that simulates the deposition process and predicts the velocity modulation algorithm needed to achieve the desired thickness profile on a given substrate surface. This process is rapidly converging and has been proven to produce the goal thickness profile on large-area substrates after only a few coating iterations.

The EUV reflectance of all AIA Mo/Si coatings was measured at beamline 6.3.2. of the ALS, as is also mentioned in Section 1. The characteristics of the beamline and its reflectometer are described in detail in Refs. 3, 4. Curved optics of up to 200 mm in diameter can be mapped in this facility. The reflectometer sample stage allows motion of an optic in 3 dimensions, tilt in 2 dimensions and azimuthal rotation of the sample holder. The detector arm can be rotated 360° around the axis of the reflectometer chamber. Once an optic is aligned, custom-designed software allows the operator to pre-calculate for each surface point a table of all coordinates of the sample stage, and program wavelength scans on multiple locations on the mirror surface without any manual input needed in-between scans. The reflectometer uses a Si photodiode detector, with an acceptance angle of 2.4°. All wavelength and reflectance results at beamline 6.3.2. were obtained within “2 $\sigma$ ” error bars of 0.05% and 0.4% relative, respectively.

Multilayer coatings for the 93.9 Å AIA channel (Mo/Y) and 303.9 Å and 335.4 Å channels (SiC/Mg) were deposited at Columbia University, using a deposition system that has been described previously in Ref. 5. In this system 50-cm-long planar cathodes are used. The spinning mirror substrate faces down and the magnetron cathodes sputter up. The individual layer thicknesses are determined by controlling the rotational velocity of the substrate as it passes over each cathode. For the coatings described here, the base pressure in the chamber was less than  $2 \times 10^{-7}$  Torr, the sputter gas (Ar) pressure was maintained at 1.6 Torr, and the cathodes were operated in constant power mode: SiC was deposited at 400 W, Mg at 400 W, Mo at 200 W and Y at 200 W.

Reflectance measurements were made using a laser plasma source reflectometer that is also described in ref W1. Reflectance measurements were made at 5 deg incidence as a function of wavelength. The sample goniometer has 5 degrees of freedom, enabling automated scans over a grid of points on figured mirror substrates as large as 30 cm in diameter. The wavelength scale of the monochromator was calibrated using multilayer samples measured at both beamline X24C at NSLS, where the AIA flight calibrations of the Mo/Y and SiC/Mg coatings will take place, and at the ALS. The reflectance accuracy (relative) of the Columbia reflectometer is approximately  $\pm 2\%$ .

## 2.2 Mo/Si multilayers

Mo/Si multilayers were selected for the 131, 171.1, 193.5, and 211.3 Å AIA channels due to the good performance of this material pair in the above wavelength range. Multilayer samples were prepared at LLNL in order to optimize the multilayer design for each channel, taking into account peak reflectance, bandwidth and out-of-band suppression as performance metrics. For this purpose, the ratio  $\Gamma$  (defined as the Mo thickness within the Mo/Si bilayer divided by the total thickness of the Mo/Si bilayer) was varied. Si wafers of 100 mm diameter, (100) orientation, 17-23 Ohm-cm resistivity, and thickness in the 515-530  $\mu\text{m}$  range, were used as substrates. The experimental results of this parametric study, including the ultimately selected  $\Gamma$  values for each channel are shown in Figure 3. It should be noted that there is a significant difference in the Mo layer microstructure between the multilayers shown in Figure 3 (a), (b), (c) (with the exception of  $\Gamma=0.23$  at 171 Å) and the multilayers in Figure 3 (d) (131 Å). The deposited Mo layer thicknesses inside the Mo/Si bilayer in the former group, for all  $\Gamma$  values considered, range from 19 Å down to 14 Å, and in this thickness range Mo forms an amorphous layer. It has been shown in the literature (Refs. 6, 7, 8) that DC-magnetron sputtered Mo films become crystalline at thicknesses above 20 Å. This is the case for all coatings shown in Figure 3 (d) (where the Mo thickness ranges from 21 Å for  $\Gamma=0.32$  to 30 Å for  $\Gamma=0.35$ ) and for the  $\Gamma=0.23$  coating in Figure 3 (c) where the Mo

thickness is about 20.3 Å, i.e. just above the amorphous-to-crystalline transition point. Amorphous Mo layers form symmetric interfaces with the Si layers inside the multilayer, while crystalline Mo forms asymmetric interfaces with Si with the Mo-on-Si interface roughness about twice the value of the Si-on-Mo interface roughness. As long as multilayers with Mo layers of thickness at exactly 20 Å are avoided (since this is the amorphous-to-crystalline transition point where the coating exhibits increased roughness), the aforementioned features of amorphous vs. crystalline Mo layers inside a Mo/Si multilayer are not expected to affect properties such as coating performance and lifetime stability of these coatings. The case of a Mo/Si multilayer with amorphous Mo layers is illustrated in Figure 4. The coating shown is the multilayer with  $\Gamma = 0.16$  which was selected for the 193.5 Å channel. The absence of any crystalline patterns in the high-resolution TEM image in Figure 4 demonstrates completely amorphous Mo and Si layers.

The lifetime properties of peak wavelength and reflectance for all above samples were monitored while the samples were maintained in laboratory, office and synchrotron environments. EUV reflectance measurements at the ALS demonstrated wavelength shifts  $\Delta\lambda \leq 0.16$  Å and relative reflectance losses  $\Delta R \leq 2$  % during the first 4 months after deposition, and no measurable changes thereafter for up to 9 months after deposition, for all samples presented in Figure 3. These results are promising in terms of meeting the AIA spec of < 10% relative reflectance loss after 5 years of operation. The properties of these Mo/Si multilayers were also tested after low-temperature, long-term annealing, keeping in mind that the AIA spacecraft has been specified to “survive” temperatures in the range from -22 °C to 52 °C. Each sample used in the annealing experiment was the center 25×25 mm<sup>2</sup> piece from a Mo/Si coated, 100-mm diameter silicon wafer. Annealing took place in a convection oven located in a cleanroom area, with pressure maintained between 0.3 – 20 Torr during annealing. After each annealing cycle, the samples were vented with N<sub>2</sub>. Four consecutive annealing steps were applied: a) 159 hours at 55 °C, b) 330 hours at 75 °C, c) 80 hours at 100 °C, and d) 76 hours at 150 °C and the EUV reflectance of each sample was measured after each annealing step. After the final annealing step at 150 °C was completed, the peak reflectivity and wavelength remained within 98 % and 99.5 % of their as-deposited values, respectively, for all Mo/Si channels. These results demonstrate that the Mo/Si coatings should be able to sustain good performance in the event of prolonged exposures at temperatures well above the maximum temperature specified for the AIA spacecraft. The results of this annealing experiment are in agreement with results from a long-term exposure of a Mo/Si sample operating at 131 Å reported in Ref. 9, and will be discussed in further detail in a future publication.

The stress properties of all multilayers in this manuscript were measured at LLNL using a FLEXUS<sup>TM</sup> stress-measuring instrument that uses a laser beam to measure the radius of curvature of the substrate before and after coating. A detailed description of the stress-measuring process is given elsewhere (Refs. 10, 11). The stress measurement results for all  $\Gamma$  values and wavelengths discussed earlier in the previous paragraph are shown in Figure 5. Mo/Si film stress has been extensively studied in the literature especially for Mo/Si multilayer coatings used in EUV lithography (see for instance Refs. 7, 10, 11, 12, 13) with bilayer thickness and  $\Gamma$  values similar or greater than the  $\Gamma$  values of the 131 Å coatings discussed in this report. The 131 Å multilayer stress results shown in Figure 5 are consistent with earlier measurements reported in the literature. To our knowledge, stress measurements for low  $\Gamma$  (0.1-0.2) Mo/Si coatings such as these shown in Figure 5 have not been previously published. Stress is compressive for all four Mo/Si AIA channel coatings plotted in Figure 5. In earlier work it has been found that in general the Mo (Si) layer contributes tensile (compressive) stress inside the Mo/Si bilayer. This conclusion is consistent with the trend of the overall compressive stress increasing with decreasing  $\Gamma$  ratio, demonstrated by the present Mo/Si multilayers. In addition to the  $\Gamma$  ratio, several other parameters such as substrate thickness, bilayer thickness and total film thickness and deposition conditions such as base and sputtering pressure may affect the net stress of a thin film. Increased stress presents a risk for multilayer optics, since it may lead to undesirable effects such as delamination of the coating from the substrate or severe figure deformation of the optic due to stress-induced competing forces between coating and substrate. Although Mo/Si coatings designed at these EUV wavelengths have successful flight heritage in missions such as the SOHO EIT, the stress shown in Figure 5 for the 211, 193.5 and 171 Å channels is considered significant and warrants further attention. We have been monitoring the stress for all coatings presented in this work and have found that stress in all samples is relaxing (i.e. moving in the tensile direction) over time. A total stress relaxation of 10-15% over periods of 200 to 300 days has been observed for all Mo/Si samples, relative to their initial stress values measured within 4 days after deposition.

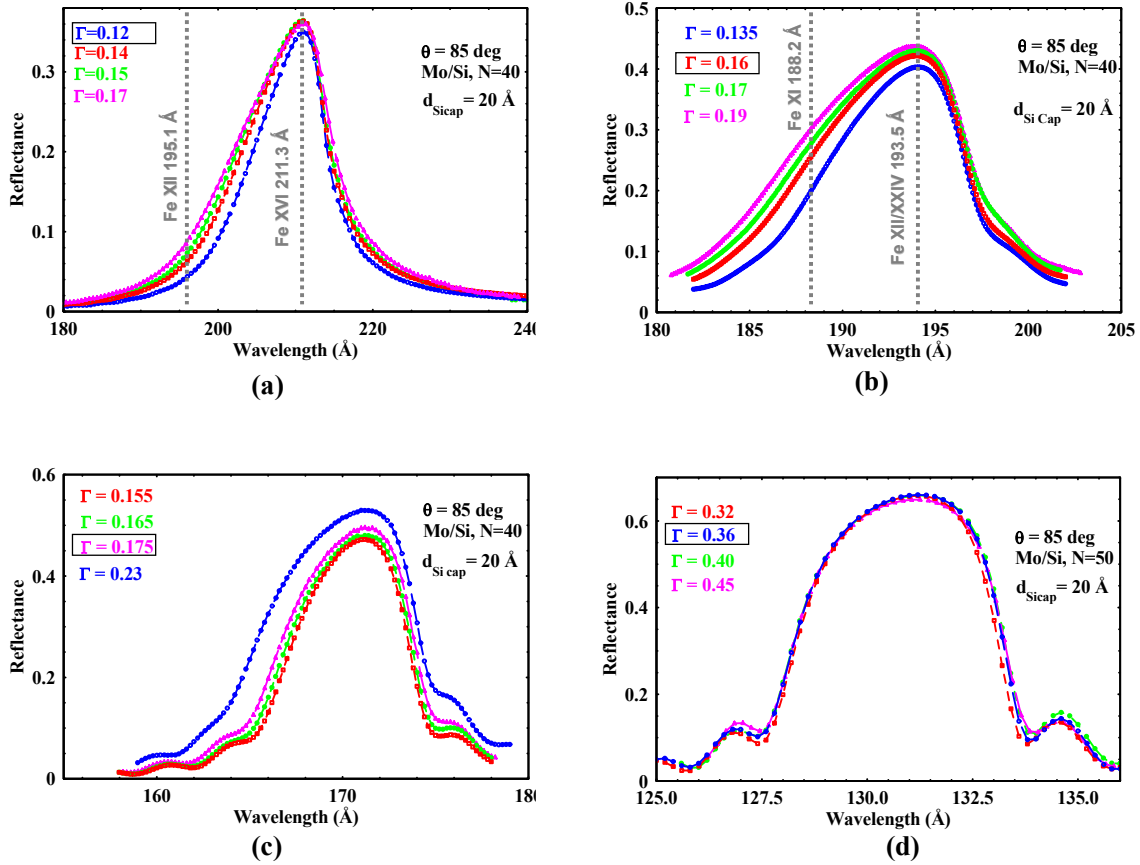


**Figure 3:**  $\Gamma$ -optimization results on Mo/Si coatings are shown for (a) 211.3  $\text{\AA}$ , (b) 193.5  $\text{\AA}$ , (c) 171.1  $\text{\AA}$  and (d) 131  $\text{\AA}$  channels. Examples of peak and out-of-band Fe ion lines are shown in (a), (b) for the 211.3 and 193.5  $\text{\AA}$  channels, respectively. The highlighted  $\Gamma$ -values indicate the selected  $\Gamma$  for each channel, and the number of Mo/Si bilayers ( $N$ ) and Si topmost layer thickness ( $d_{\text{Si cap}}$ ) are also noted in each plot. EUV reflectance measurements were performed at beamline 6.3.2. of the ALS, with the sample at  $\theta = 85^\circ$  angle of incidence, defined from the grazing direction.

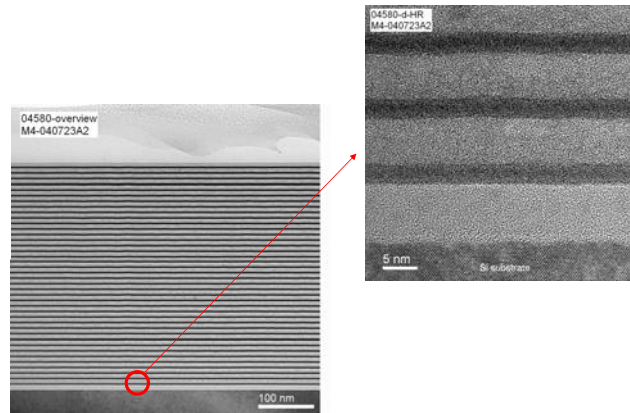


**Figure 4:** TEM images of a  $\Gamma=0.16$  multilayer selected for the 193.5 Å channel, demonstrating the amorphous structure of Si and Mo layers.

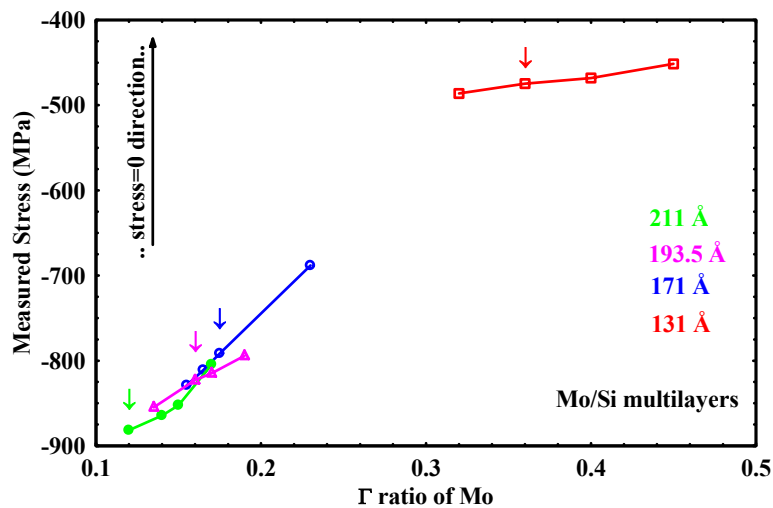


**Figure 5:** Measured stress vs.  $\Gamma$  for all Mo/Si films presented in Figure 3. The arrows indicate the selected  $\Gamma$  value for each of the four AIA channels. Stress for each film was measured within 4 days from deposition.

### 2.3 Mo/Y and SiC/Mg multilayers

Mo/Y was first developed by Montcalm *et al* (Ref. 14) and was selected for the 93.9 Å channel since it has been found (Refs. 14, 15, 16) to exhibit the best experimental performance among all material pairs in this wavelength range. Mo/Y multilayer test samples were prepared at CAL on Si wafer substrates. The fully optimized film has  $N=120$  bilayers,  $\Gamma=0.42$  (with  $\Gamma$  defined as the ratio of Mo thickness in the Mo/Y bilayer) and Mo as the topmost layer in the structure. The stress of this film was measured at LLNL, deposited on the same type of substrate and using the same apparatus and procedure as discussed in Section 2.2. Mo/Y stress was found to be less than +100 MPa (tensile), thus demonstrating inherently low (near-zero) stress for this multilayer pair.

Although SiC/Si was initially proposed (Ref. 17) for the 303.8, 335.4 Å channels, it was later found that a recently studied material pair, SiC/Mg (Refs. 18, 19, 20) could offer a factor of 2 higher reflectance and improved off-band rejection compared to SiC/Si at these wavelengths, as is shown in Figure 6(a). SiC/Mg test samples were prepared at CAL on Si wafer substrates and the experimental results of the  $\Gamma$  optimization (with  $\Gamma$  defined as the ratio of SiC thickness in the SiC/Mg bilayer) for the 335.4 Å channel are plotted in Figure 6(b). The stress of the SiC/Mg films selected for the 303.8, 335.4 Å channels was measured at LLNL, as discussed in Section 2.2, and was found to be in the +100 MPa (tensile) range, a factor of 10 lower than SiC/Si films that were initially planned for these channels.

Lifetime stability results for Mo/Y and SiC/Mg samples in ambient environment are plotted in Figure 7. Long-term annealing and proton irradiation experiments on these samples are discussed in Ref. 21.

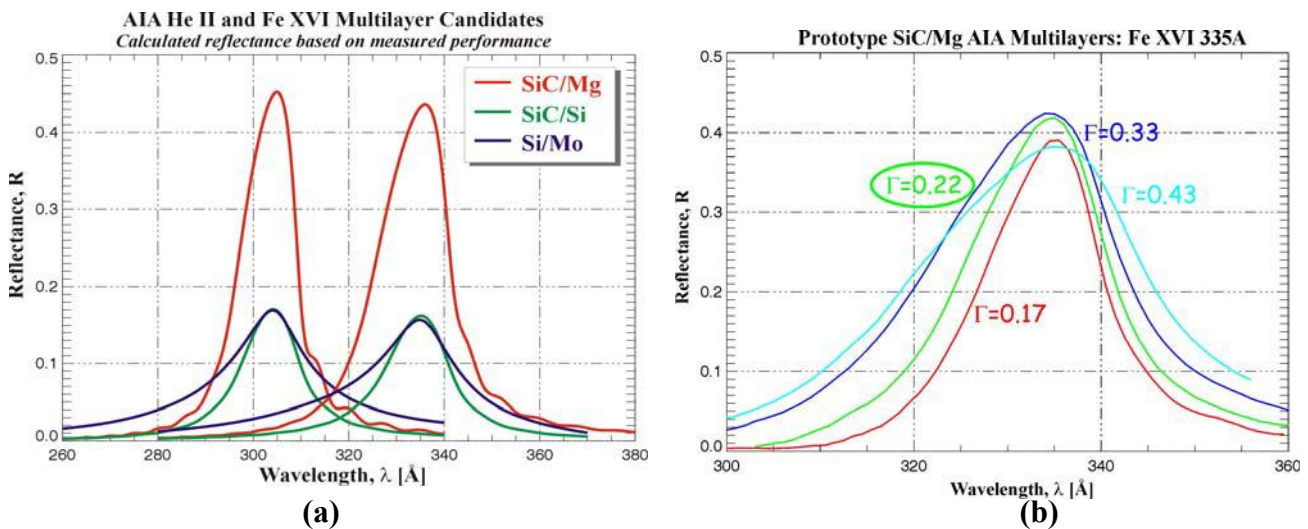


**Figure 6:** (a) Comparison of Mo/Si, SiC/Si and SiC/Mg performance at 303.8 and 335.4 Å. (b) Experimental results from the  $\Gamma$  optimization at 335.4 Å, with the selected value  $\Gamma=0.22$  highlighted. The total number of bilayers is  $N=40$  and the topmost layer in the film is SiC, for all SiC/Mg samples. All reflectance measurements were performed at the CAL facility.

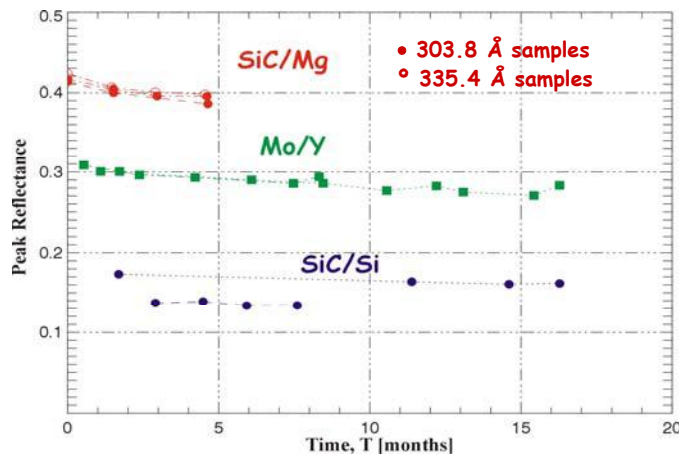


**Figure 7:** Lifetime stability results are plotted vs. time (since deposition) for the Mo/Y (93.9 Å) and SiC/Mg (303.8 and 335.4 Å) multilayers, measured at the CAL reflectometer.

## 2.4 Multilayer thickness profile results on curved AIA optics

The prescription for the primary and secondary mirror surfaces in each of the four AIA telescopes is given by

$$z(r) = \frac{1}{R} \cdot \frac{r^2}{\left[1 + \sqrt{1 - (1 + K) \cdot (r/R)^2}\right]}, \quad (1)$$

where  $z$  is the surface height,  $r$  is the radial position defined from the optical axis of each mirror,  $R$  is the radius of curvature and  $K$  is the conic constant. Table 2 summarizes the values of  $R$  and  $K$ , as well as the mirror and clear aperture (CA) radii and incidence angles for the AIA mirrors. As is noted in Table 2, the angles of incidence for both mirrors are very close to the normal direction ( $90^\circ$ ) and vary only slightly across the CA. Therefore, uniform multilayer coatings were prescribed for both primary and secondary mirrors of the AIA instrument.

	Primary (concave)	Secondary (convex)
<b>R (mm)</b>	2755.01 ± 1	1208.57 ± 0.4
<b>K</b>	-1.0916	-5.0766
<b>Mirror outer radius (mm)</b>	100.0	39.9
<b>CA outer radius (mm)</b>	94.0	34.0
<b>CA inner radius (mm)</b>	45.1	9.0
<b>Range of incidence angles within CA</b>	89.1° - 88.0°	90.4° - 91.8°

**Table 2:** AIA telescope mirror parameters. Angles of incidence are defined from the grazing direction. Optical design by W. A. Podgorski (Smithsonian Astrophysical Observatory).

The multilayer coating specification for all AIA mirrors and wavelengths requires the peak wavelength to be maintained within  $\pm 0.3$  of the bandwidth for each channel (listed in Table 1) in at least 80% of the clear aperture of each optic (listed in Table 2). We have experimentally met this specification on curved test AIA optics, for all wavelength channels. As an example, the uniformity (normalized wavelength) results from the 93.8 Å channel performed at CAL are plotted in Figure 8.

## 3. SUMMARY

We have developed multilayer coatings for the seven EUV channels of the AIA instrument (93.9, 131, 171.1, 193.5, 211.3, 303.8, and 335.4 Å) which will provide solar images with un-precedented field-of-view, temperature range, and cadence. We are anticipating a total of 8 flight substrates to be delivered at LLNL during Summer – Fall 2005, for cleaning and roughness characterization with atomic force microscopy, to verify the metrology of the substrate vendors. Multilayer coatings on the flight mirrors will be performed at LLNL and CAL, with EUV reflectance measurements at beamlines 6.3.2. of the ALS and X24C of the NSLS, respectively.

## ACKNOWLEDGEMENTS

We are thankful to Susan Ratti (LLNL) for assistance with test optics, and to Jay Ayers and Shannon Ayers (LLNL) for drawings of hardware parts. We gratefully acknowledge William A. Podgorski, Jay Bookbinder and Peter L. Smith (Harvard-Smithsonian Center for Astrophysics) for enlightening discussions and assistance. This work was performed under the auspices of the U.S. Department of Energy by the University of California Lawrence Livermore National Laboratory under Contract No. W-7405-ENG-48. Funding was provided by the Smithsonian Astrophysical Observatory.

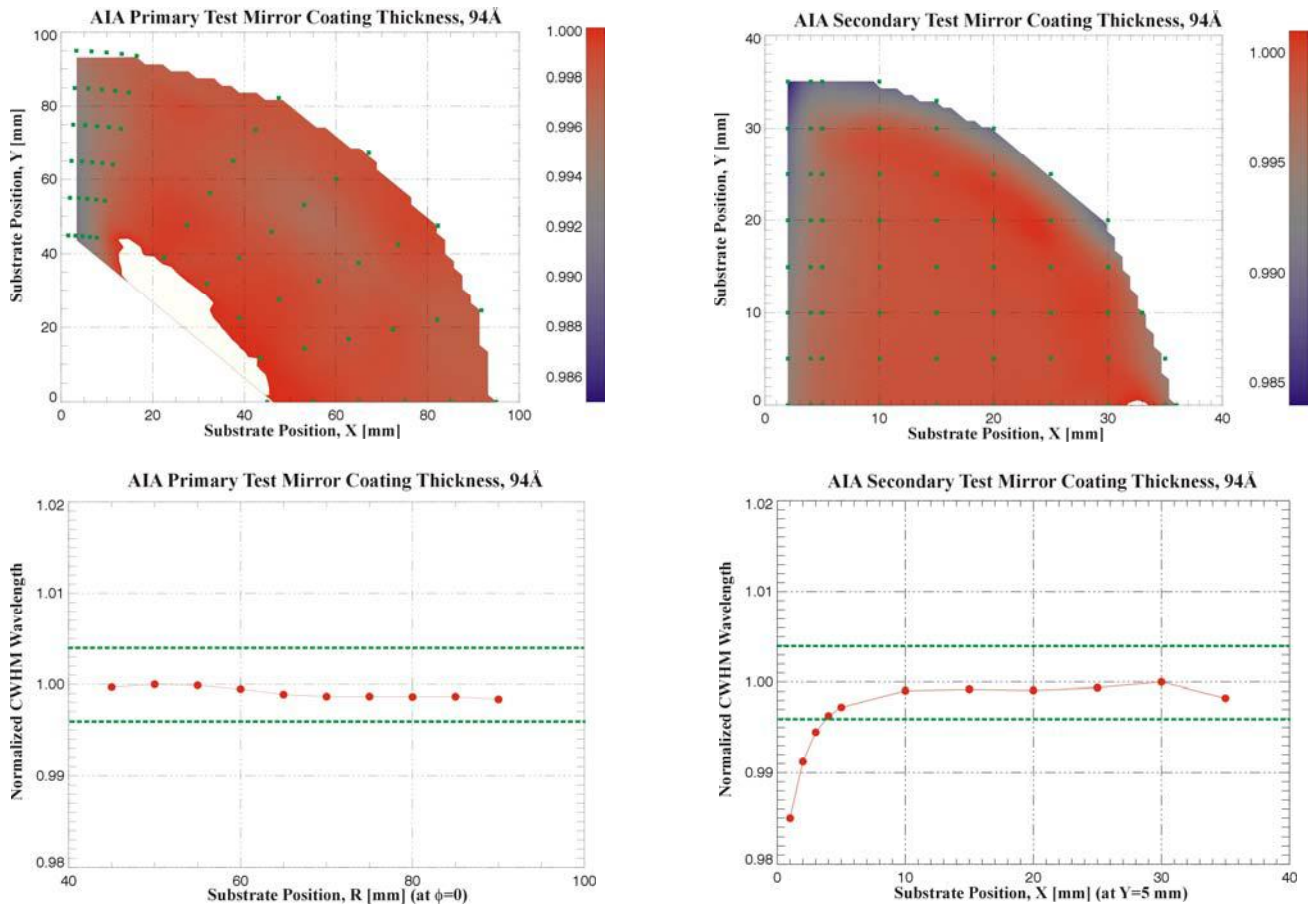


**Figure 8:** Multilayer thickness uniformity results achieved on curved, test AIA substrates (spherical approximations of the actual AIA mirrors). Demonstrated uniformity is well within the specifications (illustrated by the dotted guidelines in the bottom plots) across the CA of each mirror. The multilayer coating is Mo/Y reflecting near 93.9 Å, performed at CAL and measured with the CAL reflectometer.

## REFERENCES

1. For more information see the official SDO site at <http://sdo.gsfc.nasa.gov/> and AIA sites at <http://hea-www.harvard.edu/AIA/> and <http://aia.lmsal.com/>
2. R. Soufli, E. Spiller, M. A. Schmidt, J. C. Davidson, R. F. Grabner, E. M. Gullikson, B. B. Kaufmann, S. L. Baker, H. N. Chapman, R. M. Hudyma, J. S. Taylor, C. C. Walton, C. Montcalm, and J. A. Folta, "Multilayer optics for an extreme ultraviolet lithography tool with 70 nm resolution," in *Emerging Lithographic Technologies V*, E. A. Dobisz ed., Proc. SPIE **4343**, 51-59 (2001).
3. J. H. Underwood, E. M. Gullikson, "High-resolution, high-flux, user friendly VLS beamline at the ALS for the 50-1300 eV energy region," *J. Electr. Spectr. Rel. Phenom.* **92**, 265-272 (1998).
4. E. M. Gullikson, S. Mrowka, B. B. Kaufmann, "Recent developments in EUV reflectometry at the Advanced Light Source," in *Emerging Lithographic Technologies V*, E. A. Dobisz eds., Proc. SPIE **4343**, 363-373 (2001).
5. D. L. Windt and W. K. Waskiewicz, 'Multilayer facilities for EUV lithography', *J. Vac. Sci. Technol. B*, **12**, 3826-3832 (1994)
6. R. S. Rosen, D. G. Stearns, M. A. Villiardos, M. E. Kassner, S. P. Vernon, and Y. Cheng, "Silicide layer growth rates in Mo/Si multilayers", *Appl. Opt.* **32**, 6975-6980 (1993).
7. D. L. Windt, "Stress, microstructure, and stability of Mo/Si, W/Si, and Mo/C multilayer films", *J. Vac. Sci. Technol. A*, **18**(3), 980-991 (2000).

8. S. Bajt, D. G. Stearns, P. A. Kearney, "Investigation of the amorphous-to-crystalline transition in Mo/Si multilayers", *J. App. Phys.* **90**, 1017-1025 (2001).
9. T. Bottger, D. C. Meyer, P. Paufler, S. Braun, M. Moss, H. Mai, E. Beyer, "Thermal stability of Mo/Si multilayers with boron carbide interlayers", *Thin Solid Films* **444**, 165-173 (2003).
10. P. B. Mirkarimi, "Stress, reflectance, and temporal stability of sputter-deposited Mo/Si and Mo/Be multilayer films for extreme ultraviolet lithography", *Opt. Eng.* **38**(7) 1246-1259 (1999).
11. C. Montcalm, "Reduction of residual stress in extreme ultraviolet Mo/Si multilayer mirrors with postdeposition thermal treatments", *Opt. Eng.* **40**(3) 469-477 (2001).
12. M.E. Kassner, F. J. Weber, J. Koike, "Structural and residual stress changes in Mo/a-Si multilayer thin films with annealing", *J. Mater. Sci.* **31**, 2291-2299 (1996).
13. T. Leisegang, D. C. Meyer, A. A. Levin, S. Braun, P. Paufler, "On the interplay of internal/external stress and thermal stability of Mo/Si multilayers", *Appl. Phys. A*, 965-972 (2003).
14. C. Montcalm *et al.*, .. *Opt. Lett.* **20**, 1173-1175 (1994) ; C. Montcalm *et al.*, *Opt. Lett.* **20**, 1450-1452 (1995).
15. B. Kjornrattanawanich and S. Bajt, "Structural characterization and lifetime stability of Mo/Y extreme-ultraviolet multilayer mirrors", *Appl. Opt.*, **43**, 5955-62 (2004).
16. B. Sae-Lao and R. Soufli, "Measurements of the refractive index of yttrium in the 50-1300-eV energy region", *Appl. Opt.* **41**, 7309-7316 (2002).
17. D. L. Windt, S. Donguy, J. Seely, B. Kjornrattanawanich, "Experimental comparison of extreme-ultraviolet multilayers for solar physics", *Appl. Opt.* **43**, 5955-62 (2004).
18. Y. Kondo, T. Ejima, K. Saito, T. Hatano, M. Watanabe, "High reflection multilayer for wavelength range of 200-30 nm", *Nucl. Instrum. Meth. Phys. Res. A*, **467-468**, 333-6 (2001).
19. H. Takenaka *et al.*, *2nd International Symposium on Technologies and Applications of Photoelectron Micro-Spectroscopy with Laser-Based VUV Sources*, Tsukuba, Japan (2005).
20. I. Yoshikawa, T. Murachi, H. Takenaka, S. Ichimaru, "Multilayer coating for 30.4 nm", *Rev. Sci. Instrum.*, **76**, 066109 (2005).
21. B. Winter D. L. Windt, L. Hara, H. Lamoureux, A. Rousseau, "EUV multilayer testing for extreme solar missions" Conference Paper [5900-04], this SPIE Meeting.